Space Technology 5 multipoint observations of transpolar arc–related field-aligned currents

J. A. Cumnock,[1] G. Le,[2] S. Imber,[2] J. A. Slavin,[2] Y. Zhang,[3] and L. J. Paxton[3]

Received 6 July 2010; revised 14 November 2010; accepted 21 December 2010; published 25 February 2011.

[1] We present two transpolar arc events where for the first time we are able to analyze changes in field-aligned currents associated with high-latitude transpolar auroral arcs on time scales of a few minutes. This is accomplished through the use of highly accurate multipoint magnetic field measurements provided by the Space Technology 5 mission, which consists of three microsatellites in low-Earth orbit. In the first event we examine measurements of an arc that is part of a highly dynamic auroral pattern, that of a hook-shaped arc. In the second event, a more stable dusk oval-aligned arc is analyzed. These events illustrate the dynamic nature of arc formation and show the usefulness of high-resolution multipoint measurements. Minimum variance analysis is used to determine the appropriateness of the infinite current sheet approximation and to calculate arc alignment angles which are then compared with those estimated from UV images or precipitating particle data.

Citation: Cumnock, J. A., G. Le, S. Imber, J. A. Slavin, Y. Zhang, and L. J. Paxton (2011), Space Technology 5 multipoint observations of transpolar arc–related field-aligned currents, *J. Geophys. Res.*, *116*, A02218, doi:10.1029/2010JA015912.

1. Introduction

[2] High-latitude arcs occur as part of a variety of highly dynamic auroral configurations and are often observed during northward interplanetary magnetic field (IMF) with their formation and motion dependent on IMF B_y. These arcs may appear as single Sun-aligned arcs or as numerous arcs spread across the polar region and are typically embedded in regions of weak diffuse particle precipitation. They also vary in spatial extent and magnetospheric source regions [*Bonnell et al.*, 1999]. These arcs range in width from less than 50 km to over 1000 km where the wider arcs may also consist of thin distinct arcs [*Cumnock et al.*, 2009]. The motion of the small-scale Sun-aligned arcs is controlled by IMF B_y in the same way as large-scale transpolar arcs [*Gusev and Troshichev*, 1986; *Valladares et al.*, 1994; *Cumnock et al.*, 1997; *Kullen et al.*, 2002]. It has been proposed that small-scale Sun-aligned arcs are embedded in polar rain and thus occur on open field lines [e.g., *Carlson and Cowley*, 2005, and references therein]. In the present study we investigate only the larger-scale high-latitude arcs (>100 km width).

[3] A statistical study of high-latitude arcs by *Kullen et al.* [2002], expanding on a study by *Gussenhoven* [1982], surveyed three months of winter hemisphere Polar UVI data and found that large-scale auroral arcs located poleward of the auroral oval may be assigned to five categories: midnight (nightside originating) arcs, bending (hook-shaped) arcs, multiple arcs, oval-aligned arcs, and moving arcs. In some cases arcs are transpolar and when aligned along the noon-midnight meridian form a theta aurora [*Frank et al.*, 1982, 1986]. Single large-scale transpolar arcs aligned along the noon-midnight meridian, form almost exclusively during northward IMF. *Gussenhoven* [1982] found that these transpolar arcs show increased occurrence with increasing solar wind velocity. Moving arcs start as oval-aligned arcs that move poleward and eventually cross the entire polar region when there is an IMF B_y sign change during northward IMF [*Cumnock et al.*, 1997, 2002]; these are the longest lived (up to several hours) of the high-latitude arcs [*Kullen et al.*, 2002]. They form regardless of IMF B_x and dipole tilt [*Cumnock*, 2005] implying that this kind of transpolar arc occurs simultaneously in both hemispheres; with a dawn-dusk asymmetry and the opposite dawn-dusk motion [*Craven et al.*, 1991; *Cumnock et al.*, 2006]. Moving arcs may occur simultaneously with increased auroral oval activity such as optical substorms [*Cumnock et al.*, 2000] or auroral oval intensifications [*Blomberg and Cumnock*, 2005], and occur during times when IMF B_z makes a sudden large decrease and IMF B_y changes sign.

[4] Strong correlations between the field-aligned currents (FACs) and plasma flows associated with groups of thin distinct high-latitude arcs are seen only in the sunlit hemisphere [*Cumnock et al.*, 2009]; this is in agreement with results for FAC current dependence on hemisphere where transpolar arc luminosity is much higher in the sunlit hemisphere [*Kullen et al.*, 2008]. Convection signatures have been observed to vary a lot along the transpolar arc,

[1]Center for Space Sciences, University of Texas at Dallas, Richardson, Texas, USA.
[2]Heliophysics Science Division, NASA Goddard Space Flight Center, Greenbelt, Maryland, USA.
[3]Johns Hopkins University Applied Physics Laboratory, Laurel, Maryland, USA.

Copyright 2011 by the American Geophysical Union.
0148-0227/11/2010JA015912

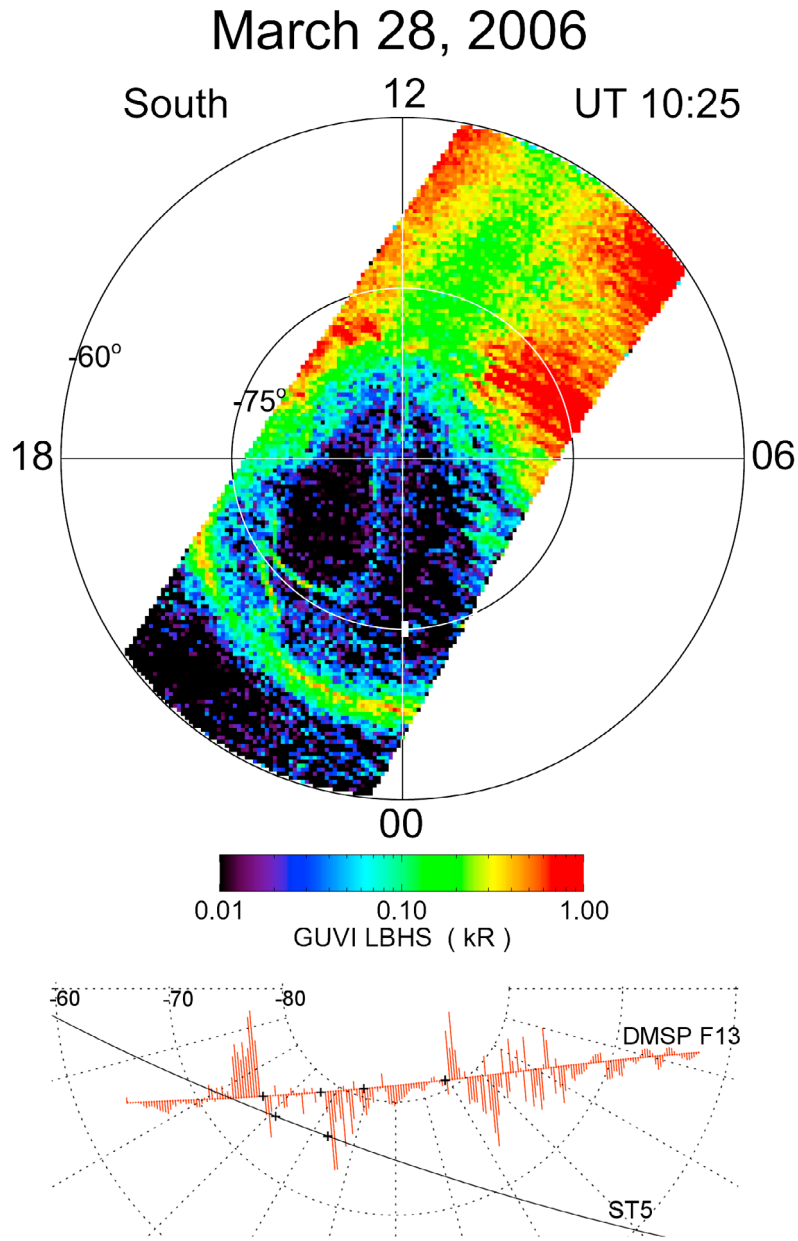

Figure 1. (top) A typical hook-shaped arc measured by TIMED GUVI during a 17 min scan of the global aurora from the Southern Hemisphere taken on 28 March 2006 centered at 1025 UT. The image is displayed in corrected geomagnetic coordinates with the Sun at the top and the lowest latitude at 60°. The pattern consists of the hook-shaped arc and oval-aligned arcs on both the duskside and dawnside, where the dawn oval-aligned arc is more separated from the oval than the dusk arc. (bottom) The ST5 satellite track (black line) and DMSP F13 cross-track plasma flows (red trace) are plotted in corrected geomagnetic coordinates. These spacecraft pass through the high-latitude arcs about 10 min prior to the GUVI measurements. The black crosses along the DMSP track correspond to the particle boundaries marked by vertical lines in Figure 2. The black crosses along the ST5 track correspond to the vertical lines in Figure 3.

from sunward to antisunward flow depending on the relative importance of the arc-associated electric field. Sunward convection (and the associated field-aligned currents) has been observed in the most intense segments of the transpolar arc [e.g., *Marklund et al.*, 1991]. Many observations of the field-aligned currents associated with TPAs indicate the existence of upward and downward current sheet pairs. A study of the relationship between the large-scale convection pattern and the transpolar arc associated field-aligned currents was performed using a numerical model by *Marklund and Blomberg* [1991]. They modeled cases with locally balanced upward and downward arc currents, as well as the case of a single upward current associated with the arc but not locally balanced. With locally balanced currents the effect

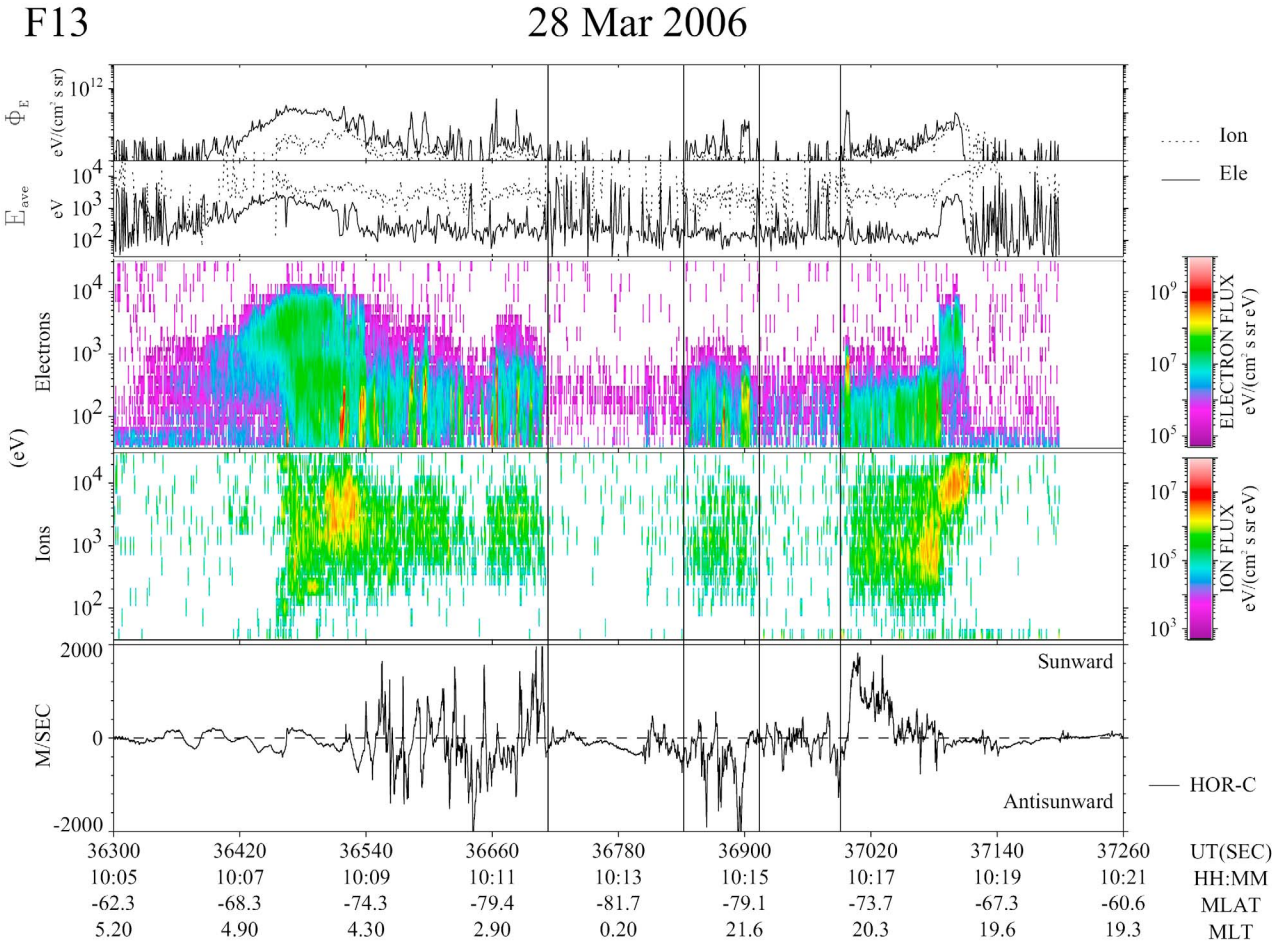

Figure 2. Data shown from a DMSP F13 pass on 28 March 2006 (1005–1021 UT) that occurs during the ST5 data period. The spectrogram includes (top to bottom) electron and ion integral energy flux, electron and ion average energy, precipitating electron spectrogram, precipitating ion spectrogram, and cross-track horizontal plasma drift. The vertical lines correspond to the black crosses shown along the DMSP satellite track in Figure 1 and mark (right to left) the poleward edge of the dusk auroral oval, the boundaries of the Sun-aligned part of the hook-shaped arc, and the poleward edge of the dawn oval-aligned arc.

on the convection pattern is localized, whereas an unbalanced arc current system leads to a modification of the convection pattern on a global scale. Satellites have observed all three current configurations [e.g., *Frank et al.*, 1986; *Menietti and Burch*, 1987; *Marklund et al.*, 1991; *Obara et al.*, 1993; *Blomberg and Marklund*, 1993; *Blomberg and Cumnock*, 2005]. Thus far observations of FACs associated with TPAs have been limited to single satellites resulting in measurements separated by large time scales (>100 min) or are limited by location of ground based measurements especially in the Southern Hemisphere (for example, magnetometer and/or convection velocity measurements).

[5] Observations indicate that transpolar arcs lie on closed field lines and have their origin in the plasma sheet or its boundary layer [*Frank and Craven*, 1988; *Peterson and Shelley*, 1984; *Craven et al.*, 1991]. Different magnetotail topologies have been proposed to explain these observations, suggesting that the tail lobes are bifurcated by closed field lines of plasma sheet origin. *Frank et al.* [1982, 1986] describe the tail plasma sheet as bifurcated such that a plasma sheet bulge extends into the lobes, which is consistent with observations of midnight originating arcs. *Huang et al.* [1987, 1989] showed that a filamentary extension of the plasma sheet into the lobes may be responsible for the plasma sheet bifurcation and is consistent with observations of transpolar arcs. There are two types of conceptual magnetospheric models that attempt to explain transpolar arc formation: dayside merging and magnetotail twisting, both of which depend on IMF orientation. *Kan and Burke* [1985] and *Toffoletto and Hill* [1989] showed that merging (based on the antiparallel merging model of *Crooker* [1979]) near the cusps during northward IMF produces two regions of open flux along the flanks of the tail magnetopause, separated by a central channel of plasma sheet that spans the magnetotail from north to south. These models do not explain the dawn-dusk motion observed in oval-aligned and moving arcs and the influence of IMF B_y; however, they do account for the formation of midnight originating arcs and may play an important role in the formation of hook-shaped arcs. Many observed features of TPAs may be explained by

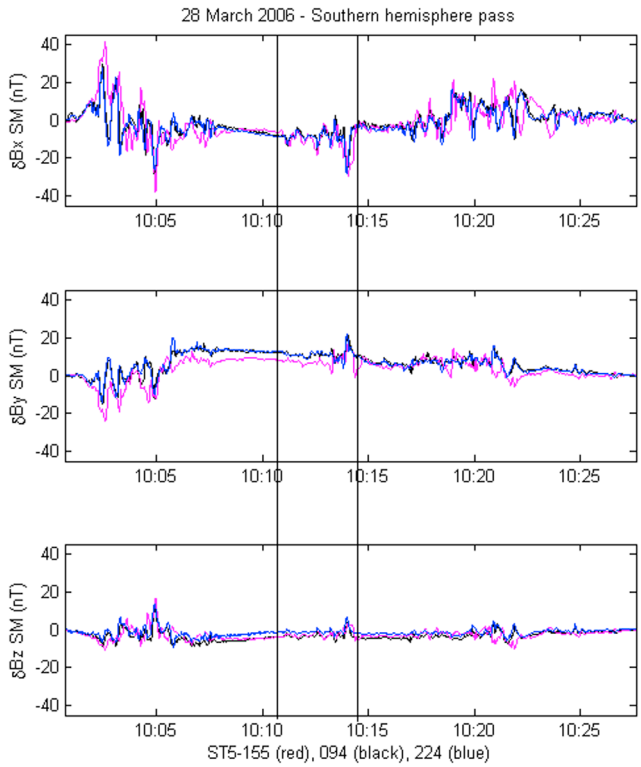

Figure 3. Time-shifted components of the ST5 magnetic field variations in the Southern Hemisphere (1000–1028 UT) plotted in solar magnetic coordinates taken at about the same time as data available from DMSP F13 (Figure 2) and 10 min prior to the GUVI image (Figure 1). The leading (ST5-155, red trace) and trailing (ST5-224, blue trace) spacecraft are shifted in time (162 and 24 s with respect to the center satellite ST5-094, respectively) so that measurements taken at the same location are aligned. The time shown is that of the center satellite, ST5-094 (black trace).

IMF rotations which cause magnetotail twisting; where arcs move poleward when the near earth and far tail portions of the magnetotail are twisted in opposite directions [*Kullen*, 2000]. MHD simulations of magnetotail twisting partially replicate observations of oval-aligned and moving arcs; where a moving Sun-aligned arc maps to a bar of closed field lines [*Slinker et al.*, 2001; *Kullen and Janhunen*, 2004]. However, in these simulations the polar cap is not entirely bifurcated by closed field lines and these simulations do not explain how field-aligned currents are generated in the tail. *Naehr and Toffoletto* [2004] analyzed results from both antiparallel merging and tail twist models and determined that transpolar arc formation and evolution are primarily magnetotail twisting but they also do not obtain a complete bifurcation of the polar cap. Thus it is assumed that at least two types of drivers, magnetotail twisting and dayside merging, are necessary for high-latitude arc formation.

[6] These high-latitude auroral phenomena are all very dynamic and change significantly (both spatially and in intensity) on time scales much faster than the ~100 min orbital period of low-Earth orbit satellites like DMSP. In the present study we use data from the Space Technology 5 (ST5) mission consisting of three microsatellites which provide the first multipoint measurements of field-aligned currents in low-Earth orbit (~300–4500 km) [*Slavin et al.*, 2008]. We examine the FACs associated with high latitude arcs using ST5 because they give us three highly accurate measurements of the FACs with temporal spacing of ~1–10 min which enable us for the first time to analyze variations in high-latitude arcs on short time scales. Spatial and temporal changes in TPAs on these time scales are not possible to observe with single satellites in low-Earth orbit and thus are not well understood or examined. Minimum variance analysis (MVA) is used to estimate the arc aligned angles in the sunward direction which are then compared with those estimated from UV images or precipitating particle data in order to determine the validity of using FACs to estimate transpolar arc alignment.

2. Observations and Discussion

[7] The three ST5 satellites provide highly accurate magnetic field measurements during a three month period. The satellites follow the same trajectory and their separation varies between 5000 and 50 km. The ST5 magnetometers (MAG) provide 16 vectors per second to the spacecraft command and data handling system [*Slavin et al.*, 2008]. These instruments have two ranges: ±64,000 and ±16,000 nT that are controlled by the individual satellites using the measured magnetic field strength. The digital resolution of the MAG is 1.25 nT and 0.30 nT, respectively, in its high and low field ranges. The intrinsic noise for these miniature magnetometers was less than 0.1 nT RMS at 1 Hz. Prelaunch testing in the Goddard Space Flight Center Magnetic Coil Facility showed that stray magnetic fields due to the satellite at the MAG sensor are less than 1 nT [*Slavin et al.*, 2008]. The MAG data processing is described in the *Wang et al.* [2009] statistical study of field-aligned current sheet motion using the multispacecraft Space Technology 5 observations. The instrument gains and offsets changed by less than 0.1% over the course of the mission and no evidence of contamination due to stray satellite magnetic fields has been found [*Slavin*, 2006].

[8] The 105.6° inclination orbit of 300 to 4500 km has a period of 136 min, resulting in a few orbits per day when the track is in an optimal location for passing through high-latitude arcs, that is, on the nightside of the dawn-dusk meridian which in this case occurs in the Southern Hemisphere. The three spacecraft follow the same trajectory separated by 3 to 10 min. Thus, they cross the FAC region successively and their magnetic field profiles should be the same (if shifted in time) if the magnetic variations are all spatial and the FAC structures do not have any temporal variation. Since the high-latitude arcs must be identified by UV images and/or precipitating particle measurements, we are limited by the lack of imagers during the ST5 mission which are capable of taking multiple images during each polar pass. For the two events presented TIMED GUVI is available only for the first event. The GUVI cross-track FUV (115 to 180 nm) scanning imaging spectrograph provides one horizon-to-horizon image per polar pass, made during a 17 min period. The DMSP satellites have a Sun-synchronous circular polar orbit where the satellite track is aligned approximately along the dawn-dusk or ~9 to 20 MLT meridians. The SSJ/4 instrument includes curved

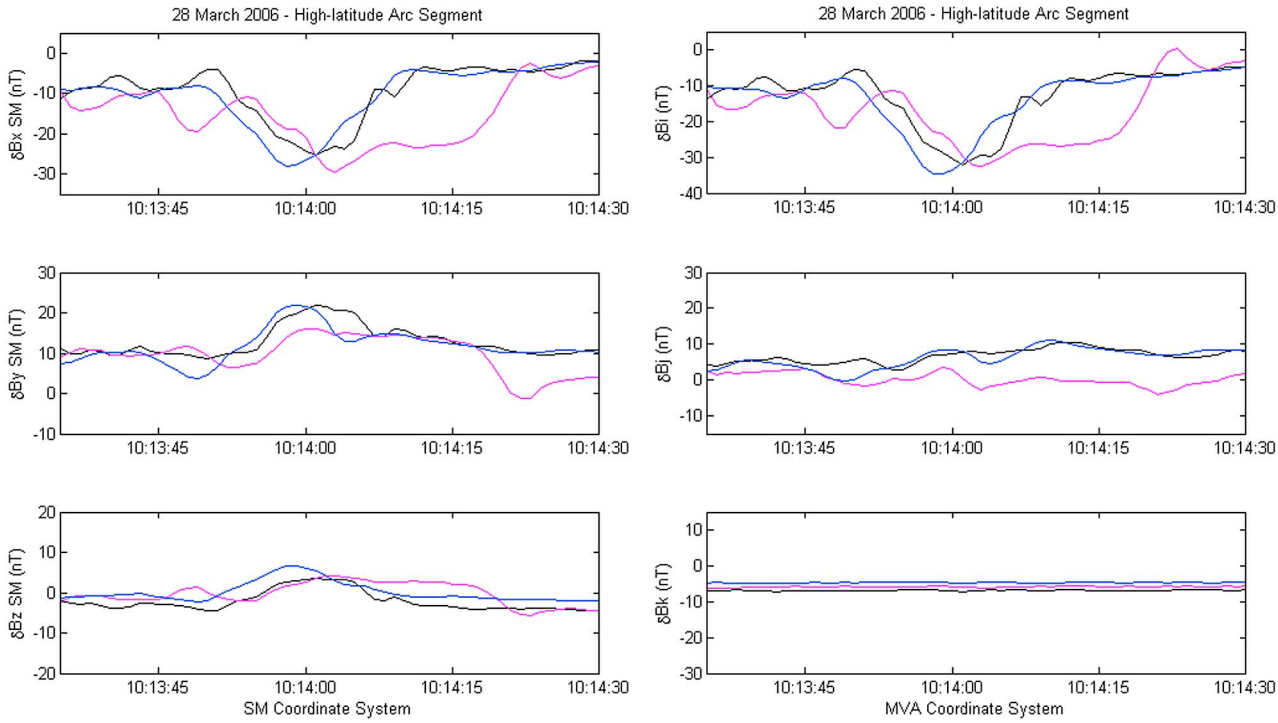

Figure 4. Time-shifted ST5 magnetic field variations associated with the dusk oval-aligned arc (right quarter of the region marked by vertical lines in Figure 3) plotted in (left) SM coordinates and (right) MVA coordinates. The leading (ST5-155, red trace) and trailing (ST5-224, blue trace) spacecraft are shifted in time so that measurements taken at the same location are aligned. The time shown is that of the center satellite, ST5-094 (black trace).

plate electrostatic analyzers to measure electrons and ions from 32 eV to 30 keV at a rate of one complete electron and ion spectrum per second resulting in a spatial resolution of about 7 km. The SSIES instrument provides measurements of the horizontal plasma flow and ion density at a rate of 6 samples per second. In addition to ST5, for both events multiple satellite data are available.

[9] We here present two examples of high-latitude arc and auroral oval associated field-aligned currents where the currents are expected to change temporally or spatially corresponding to changes in the interplanetary magnetic field. We are able to observe large-scale, mesoscale and small-scale changes in the magnetic fields (~1000, ~150 and <150 km, respectively). The two ST5 events shown occur during quiet times and thus have much weaker FACs than those measured during geomagnetic storms [*Le et al.*, 2009]. The first event occurs when the ST5 spacecraft are within 3 min of one another measuring part of a highly variable high-latitude arc pattern; in the second they are spread apart by 11 min and make measurements of the more slowly evolving oval-aligned arc. Thus, we can analyze temporal variations within these time scales.

[10] In analyzing the magnetic field data we treat the large-scale FACs as infinite planar sheets. Using this approximation we expect the magnetic field variations associated with a transpolar arc to be locally aligned with the Sun-aligned direction. The infinite sheet assumption is not appropriate when the spacecraft crosses an actual finite length current sheet near one of its ends where the magnetic field perturbation will not be confined to one component. To determine the direction along which the magnetic field variation is at a minimum we use minimum variance analysis (MVA) [*Sonnerup and Cahill*, 1967; *Sonnerup and Scheible*, 1998]. The MVA also allows us to evaluate the applicability of the infinite sheet assumption.

[11] The minimum variance analysis consists of finding the three eigenvalues and corresponding eigenvectors of the covariance matrix of the magnetic field. The eigenvector corresponding to the smallest eigenvalue represents the direction of minimum field variance. Similarly, the eigenvector corresponding to the largest eigenvalue represents the direction of maximum variance. The third eigenvector completes an orthogonal coordinate system, the MVA system. In the MVA coordinate system, $\boldsymbol{i}$, $\boldsymbol{j}$, and $\boldsymbol{k}$ are defined to be the maximum, intermediate, and minimum variance directions, respectively. In regards to field-aligned currents, the coordinate $\boldsymbol{k}$ is also the field-aligned direction and $\boldsymbol{i}$ and $\boldsymbol{j}$ are the two directions transverse to the magnetic field. Magnetic field variations exclusively in the $\boldsymbol{i}$ direction indicate an infinite and homogeneous current sheet; the current sheet normal direction would then be along the $\boldsymbol{j}$ direction. For the more realistic case with magnetic field variations in both transverse directions, the ratio of the maximum and intermediate variance eigenvalues (e_i/e_j) indicates how much variation is in one direction. If the spacecraft is close to the end of a finite current sheet we would expect to see magnetic field variations in both the $\boldsymbol{i}$ and $\boldsymbol{j}$ directions. Thus we can ascertain the validity

Table 1. MVA Results for the Dusk Oval-Aligned Arcs on 28 March 2006 and 20 April 2006[a]

Date	Spacecraft	e_i/e_j Ratio	Angle of Current Sheet With Sun-Aligned Direction
28 Mar 2006	ST5-155	26	33
	ST5-094	17	29
	ST5-224	8	26
20 Apr 2006	ST5-094	21	22
	ST5-224	20	21

[a]The satellites are ordered by time, with the leading spacecraft first. The e_i/e_j ratio and the angle of the current sheet with respect to the Sun-aligned direction are given for each event and spacecraft. A large ratio of the maximum to intermediate variance eigenvalues (e_i/e_j) indicates that the FACs can with some confidence be approximated by infinite current sheets. Comparison with the Sun-aligned direction is appropriate for high-latitude transpolar arcs which are often observed to be Sun aligned.

of the infinite current sheet approximation for the large-scale currents associated with both the auroral oval and high-latitude arcs first by looking at the ratio of the maximum and intermediate variance eigenvalues (e_i/e_j). The larger the ratio of the maximum to intermediate variance eigenvalues (e_i/e_j) we can with more confidence assume the FACs can be approximated locally by infinite current sheets. We then also calculate how closely the current sheets are Sun aligned.

2.1. Event 1: Hook-Shaped Arc, 28 March 2006

[12] Hook-shaped arcs are usually short lived, faint and highly variable. They originate as poleward moving transpolar arcs where one end of the arc separates from the main oval and moves toward the other side of the oval whereas the other end remains fixed [*Ismail and Meng*, 1982; *Murphree et al.*, 1982; *Gusev and Troshichev*, 1986; see also *Kullen et al.*, 2002]. These arcs occur during average northward IMF conditions and start to occur typically in connection with a short southward IMF B_z time period [*Kullen et al.*, 2002]. In our case, a short southward IMF B_z time period occurs at 0945 UT, about 35 min before the GUVI image is taken and where the arc has already moved considerably poleward. It is often the case that an oval-aligned transpolar arc is seen simultaneously on the opposite side of the oval.

[13] Figure 1 (top) shows a hook-shaped arc measured during a 17 min scan of a TIMED GUVI global aurora image from the Southern Hemisphere taken on 28 March 2006 where the time shown (1025 UT) denotes the midpoint of the scan. The image is displayed in Altitude Corrected geomagnetic coordinates (AACGM) (see *Baker and Wing*

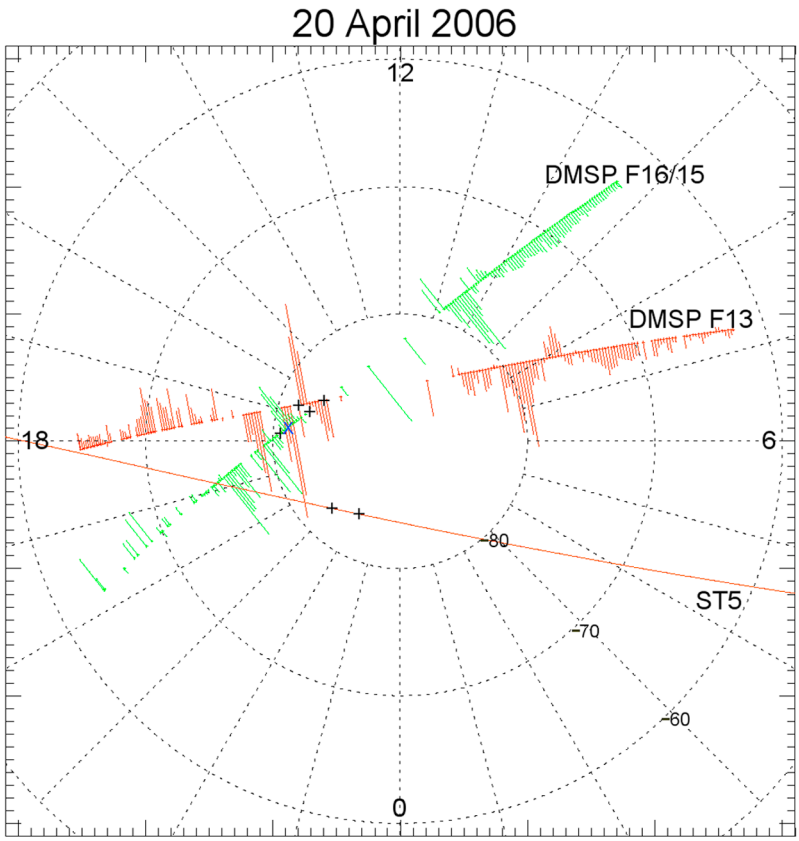

Figure 5. Polar plot with the ST5 satellite track (red line) and DMSP F13 (red trace) and F16/15 (green trace) cross-track plasma flows plotted in corrected geomagnetic coordinates from 20 April 2006. DMSP F16 has the same track as F15 but precedes F15 by 9 min. The blue cross on the DMSP F16/15 satellite track corresponds to the poleward edge of the expanded duskside oval marked by the vertical line in Figure 6; the black crosses along the DMSP tracks correspond to the particle boundaries associated with the high-latitude arc marked by vertical lines in Figures 7 and 8. The black crosses along the ST5 track mark the boundary of the FAC pair and correspond to the vertical lines in Figure 9.

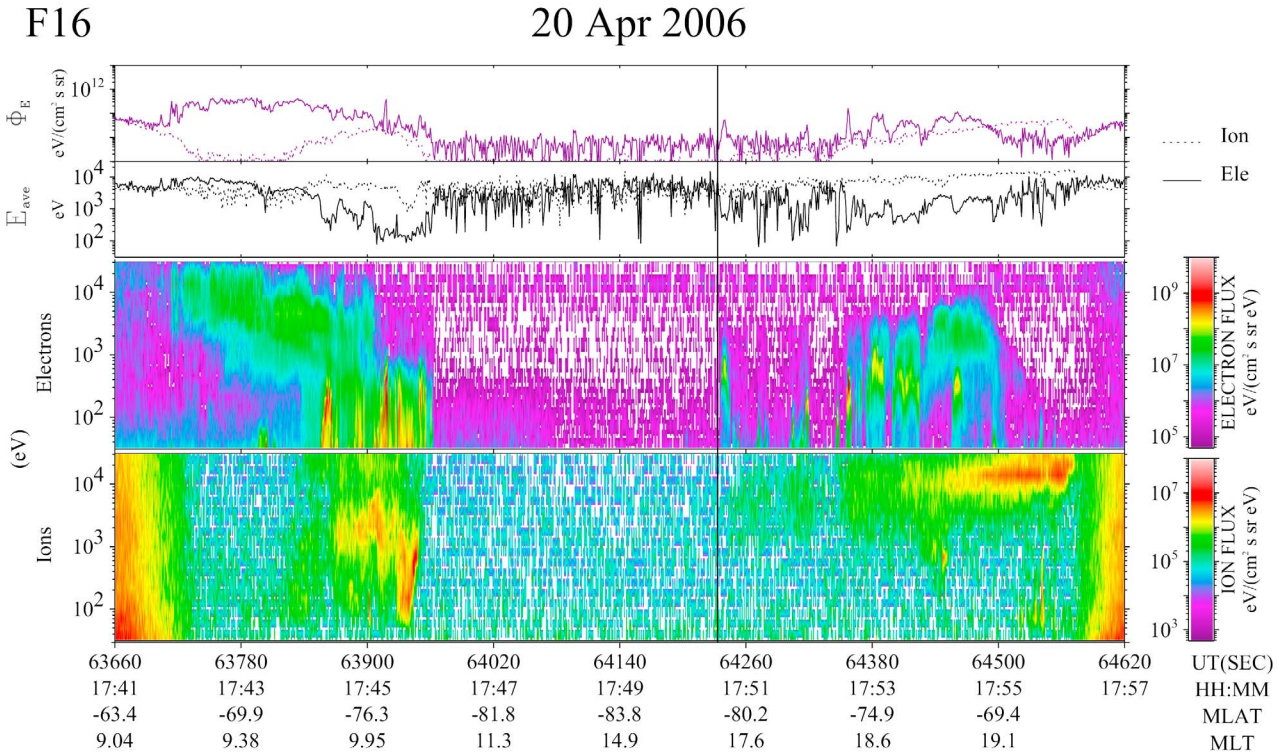

Figure 6. Data shown from a DMSP F16 pass on 20 April 2006 (1741–1757 UT), which occurs during the ST5 time period. The spectrogram includes (top to bottom) electron and ion integral energy flux, electron and ion average energy, precipitating electron spectrogram, and precipitating ion spectrogram. Cross-track horizontal plasma drift data are not available for this pass. The spectrogram shows an expanded duskside oval (right side of plot) with a thin region of energetic particles at the poleward edge. The vertical line corresponds to the blue cross shown along the DMSP satellite track in Figure 5 and marks the poleward edge of the expanded dusk auroral oval.

[1989] for details) with the Sun at the top and the lowest latitude at 60°. It is common to see such faint large-scale arcs during northward IMF. The pattern shown in Figure 1 consists of the hook-shaped arc and oval-aligned transpolar arcs on both the duskside and dawnside, although the dawn oval-aligned arc is only partially seen in the image. The Sun-aligned part of the hook-shaped arc is aligned along the duskside of the noon-midnight meridian and is attached to the dayside of the auroral oval. The other end of the hook-shaped arc is attached to a dusk oval-aligned arc. The poleward edge of the dawn oval-aligned arc is at higher latitudes than the poleward edge of the dusk oval-aligned arc. We note that a hook-shaped arc is seen also in the Northern Hemisphere (GUVI data not shown) on the dawnside of the noon-midnight meridian, which is the expected dawn-dusk asymmetry between hemispheres resulting from IMF B_y influence on high-latitude auroral arcs.

[14] Figure 1 (bottom) shows the nightside of a polar plot with the ST5 satellite track and DMSP F13 cross-track plasma flows (red). These measurements are made about 10 min prior to the time period of the GUVI image in Figure 1 and thus, because of the dynamic nature of the hook-shaped arc, we do not expect the arc signatures measured by the different satellites to be colocated. The Sun is toward the top, magnetic local time is denoted by the dashed lines and the lowest latitude is at 60°. The black crosses along the DMSP track correspond to the particle boundaries marked by vertical lines in Figure 2. These lines mark (from left to right in Figure 1) the poleward edge of the expanded dusk oval, the boundaries of the high-latitude arc and the poleward edge of the dawn oval-aligned arc. The black crosses along the ST5 track mark where the spacecraft passes through the nightside of the hook-shaped arc and dusk oval-aligned arc and correspond to the vertical lines in Figure 3. Because of the variability of the arc and the 10 min time delay between ST5/DMSP and GUVI, all of the emission regions are not aligned. In the GUVI image the hook-shaped arc appears to have moved to slightly higher latitudes and the dusk oval-aligned transpolar arc to lower latitudes since the DMSP measurements were taken.

[15] Figure 2 shows data from a Southern Hemisphere DMSP F13 pass in the dawn-to-dusk direction corresponding to the DMSP orbit track in Figure 1 and occurs about 10 min prior to the GUVI image. Figure 2 includes, from top to bottom, electron and ion integral energy flux, electron and ion average energy, electron differential energy flux spectrogram, ion differential energy flux spectrogram, and cross-track horizontal plasma drift. The vertical lines correspond to the black crosses shown along the DMSP satellite track in Figure 1. DMSP F13 passes through the dawnside of the expanded oval (left side of Figure 2) from which the poleward edge has separated forming an oval-aligned transpolar arc. The dawnside oval has remained

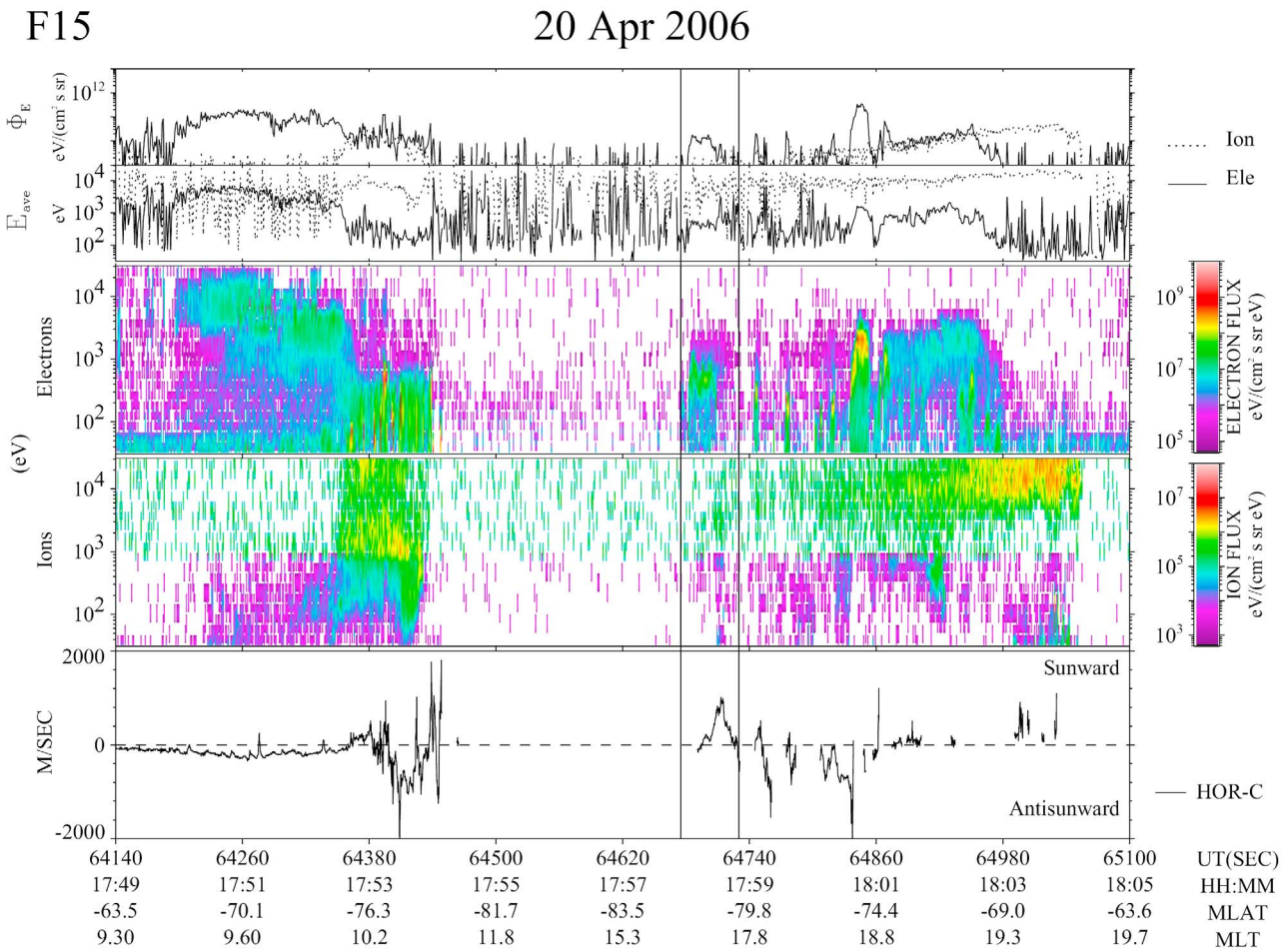

Figure 7. Data shown from a DMSP F15 pass on 20 April 2006 (1749–1805 UT). These DMSP measurements are closest in time to the high-latitude arc measured by ST5 and occur about 9 min after F16 but along the same satellite track. The spectrogram includes (top to bottom) electron and ion integral energy flux, electron and ion average energy, precipitating electron spectrogram, precipitating ion spectrogram, and cross-track horizontal plasma drift. The vertical lines correspond to the black crosses shown along the DMSP satellite track in Figure 5 and mark the boundaries of the dusk oval-aligned arc.

relatively stable in the 10 min between the DMSP and GUVI passes, thus, the poleward edge of the expanded oval is roughly aligned in both the UV and the particle data. However, the small gap which exists between the dawn transpolar arc and oval in the DMSP spectrogram is not apparent in the GUVI image. On the duskside of the noon-midnight meridian (right side of Figure 2) DMSP F13 passes through both the Sun-aligned part of the hook-shaped arc and the duskside oval. In this case in the 10 min between the DMSP and GUVI measurements the hook-shaped arc has moved poleward and thus measurements are not aligned with GUVI. In addition, the poleward edge of the dusk oval has evolved from an enhancement in the DMSP precipitating particles to a separated dusk oval-aligned arc as seen in the GUVI image.

[16] The Sun-aligned part of the hook-shaped arc (marked by the two center vertical lines in Figure 2) is colocated with antisunward flow on the duskward part (right side of Figure 2) and reduced antisunward flow on the dawnward part (left side of Figure 2) corresponding to a pair of FACs (not shown). In this case the convection associated with the Sun-aligned part of the arc is not locally balanced and thus may affect the large-scale convection. However, the global ionospheric plasma drift pattern is very structured with no coherent large-scale pattern, thus it is difficult to determine if the arc has modified the convection pattern on a global scale. The subsequent Southern Hemisphere DMSP pass (not shown) shows that the hook-shaped arc has almost completely faded by about 1200 UT. The Northern Hemisphere pass is at too low latitudes on the dayside to detect high-latitude arcs.

[17] Figure 3 shows ST5 magnetic field measurements from the Southern Hemisphere taken at about the same time as data available from DMSP F13 (Figure 2) and 10 min prior to the GUVI image (Figure 1). The time-shifted components of the ST5 magnetic field variations are plotted in solar magnetic (SM) coordinates, with the background IGRF geomagnetic field subtracted and the endpoints shifted to zero. The data have a time resolution of 1 s which are spin averaged (with a spin period of ~3 s) with overlapping averaging windows. The leading (ST5-155, red trace) and trailing (ST5-224, blue trace) spacecraft are shifted in time

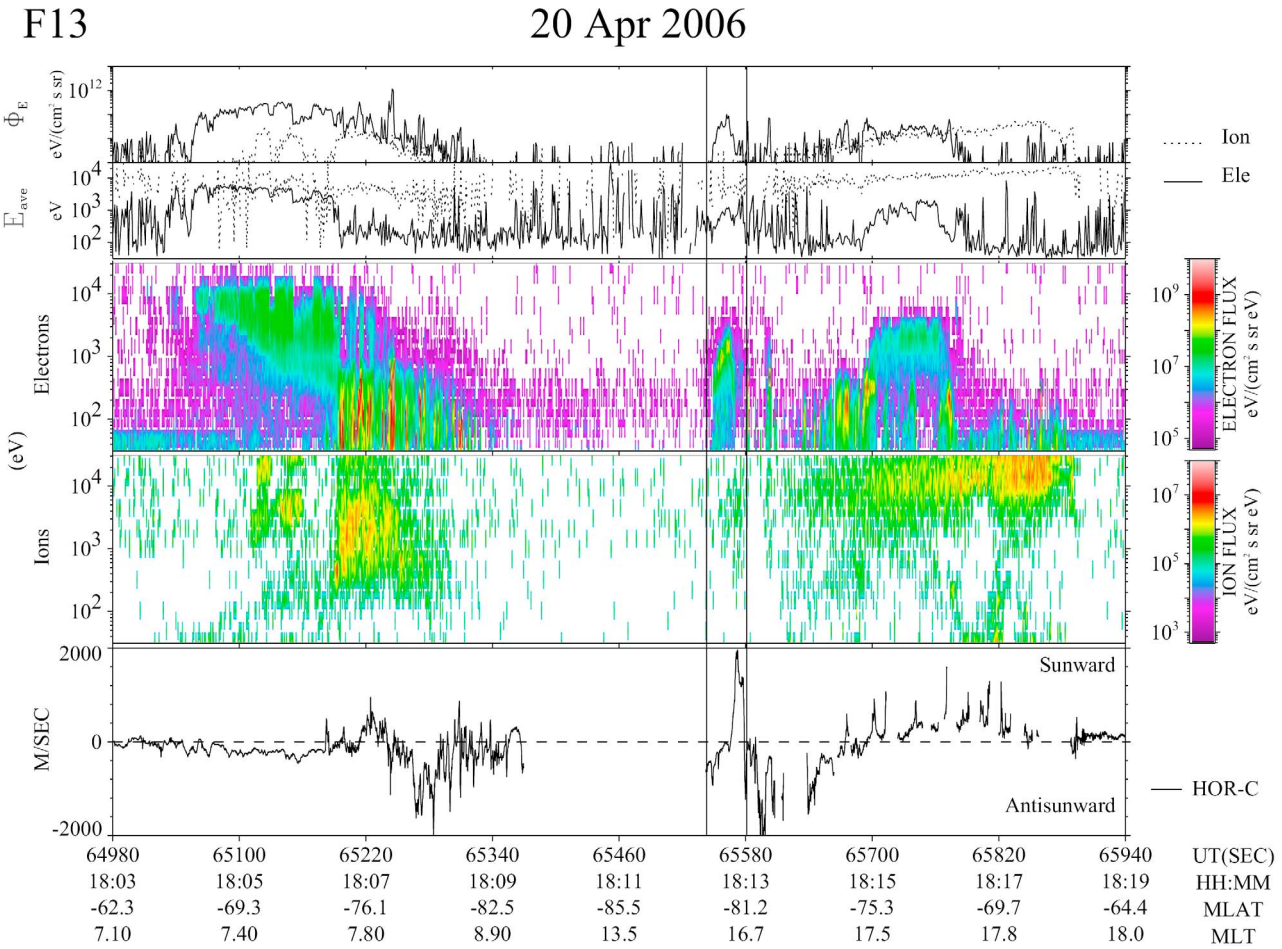

Figure 8. Data shown from a DMSP F13 pass on 20 April 2006 (1803–1819 UT) in the same format as Figure 7. The vertical lines correspond to the black crosses shown along the DMSP F13 satellite track in Figure 5 and mark the boundaries of the dusk oval-aligned arc.

(162 and 24 s with respect to the center satellite ST5-094, respectively) so that measurements taken at the same location are aligned. The time shown is that of the center satellite, ST5-094 (black trace).

[18] The gradients in δB_x correspond to field-aligned currents, assuming that the currents may be approximated by Sun-aligned sheets. Positive slope corresponds to upward FACs and negative slope to downward. Most of the magnetic field variations are in the δB_x component (~80 nT); however variations along the dawn oval (left side of Figure 3) in the δB_y and δB_z directions are also fairly large (~30 nT). Field-aligned currents associated with the auroral oval are seen on the left (dawn) and right (dusk) sides. The maximum perturbations are much less than those seen at these altitudes during active periods, during which values of ~1000 nT are more typical [e.g., see *Le et al.*, 2009]. The magnetic field measurements corresponding to the nightside portion of the hook-shaped arc and the dusk oval-aligned arc are marked by two vertical lines which correspond to the black crosses on the ST5 satellite track in Figure 1. Even though this region consists of multiple upward and downward directed mesoscale currents, there is very little temporal variation during the 3 min between leading and trailing ST5 satellites. However, fairly large temporal variations are seen in the measurements corresponding to the auroral oval, especially on the duskside (right side of Figure 3). These variations occur during the ~162 s separation between ST5-155 and ST5-094.

[19] The magnetic field variations associated with the dusk oval-aligned arc are displayed in both SM and MVA coordinates in Figure 4. These measurements also correspond to the right quarter of the region marked by vertical lines in Figure 3. The large-scale magnetic field variations are seen mainly in the δB_i component, while δB_j contains mostly mesoscale variations. All three ST5 satellites measure a pair of field-aligned currents associated with the dusk oval-aligned arc. Only mesoscale changes occur during the ~30 s between ST5-094 and ST5-244. Large-scale changes are seen between ST5-155 and the two following spacecraft. During this 2.5 min time period the current pair has narrowed by ~50%. It is only the upward current which has narrowed, and since it retains about the same magnitude this means that the current density is increasing and thus auroral arc luminosity may also increase. This assumption could be verified if we had multiple consecutive UV images (or precipitating particle data) on these time scales, and could observe a dusk oval-aligned arc which intensifies as it separates from the oval.

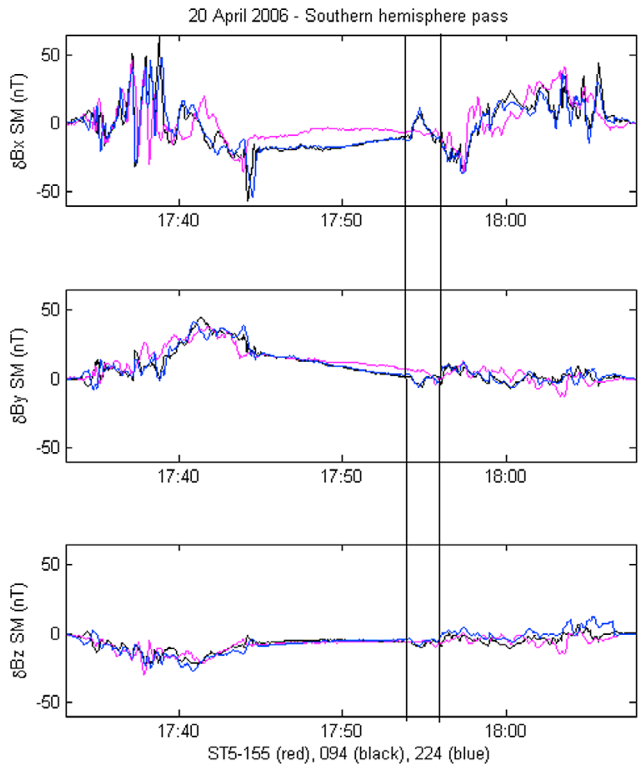

Figure 9. Time-shifted components of the ST5 magnetic field variations in the Southern Hemisphere (1733–1808 UT) plotted in solar magnetic coordinates taken at about the same time as data available from DMSP F16, F15, and F13. The leading (ST5-155, red trace) and trailing (ST5-224, blue trace) spacecraft are shifted in time so that measurements taken at the same location are aligned. The time shown is that of the center satellite, ST5-094 (black trace). The vertical lines correspond to the black crosses shown along the ST5 satellite track in Figure 5 and mark the boundaries of the dusk oval-aligned arc.

[20] The ratios of the maximum and intermediate variance eigenvalues (e_i/e_j) and the angles the dusk oval-aligned arc makes with the Sun-aligned direction are listed in Table 1. In temporal order (ST5-155, ST5-094 and ST5-224) they are 26, 17 and 8. Such large ratios indicate that an infinite current sheet approximation is adequate for our purposes. The angles the arc makes with the Sun-aligned direction are also given and are consistent with those of a dusk oval-aligned arc. The nightside portion of an oval-aligned arc may tilt either positive or negative with respect to the Sun, with positive tilt more commonly observed. On the duskside of the noon-midnight meridian, positive orientation is where the arc is angled away from noon as is observed in this case. Not only has the arc decreased in width between ST5-155 and ST5-094, the angle of the current sheet with the Sun-aligned direction is also decreasing in time. The result of this motion is seen in the GUVI image 10 min later. This change is consistent with the variability observed in the aurora associated with hook-shaped arcs. As discussed earlier, for the hook-shaped arc pattern, the changes in the merging region are thought to cause the deformation of the arc. Multiple events with measurements on ST5 time scales may provide insight into the importance of magnetic merging and magnetotail twisting in the formation of the hook-shaped arc.

[21] The portion of the arc currents (left portion of the region marked by vertical lines in Figure 3) where ST5 passes along the nightside part of the hook-shaped arc cannot be assumed to represent a current sheet and thus is not appropriate for MVA. As already mentioned, the largest variations between ST5 spacecraft measurements are in the auroral ovals. MVA confirms this with low e_i/e_j ratios, with the lowest being associated with the dusk auroral oval (3, 3, 2), indicating that the FACs are not sheet-like structures or that the spacecraft has crossed the finite length current sheet near the end such that the magnetic field perturbation is not confined to only one sheet-aligned component.

2.2. Event 2: Dusk Auroral Oval-Aligned Transpolar Arc, 20 April 2006

[22] Oval-aligned arcs [*Murphree and Cogger*, 1981] usually appear near the dawn or duskside oval and may become separated from the auroral oval before they fade. They are a common northward IMF phenomenon persisting from tens of minutes up to hours. When oval-aligned arcs occur on both sides of the auroral region (usually during very small IMF B_y) the pattern is called "horse collar" aurora [*Hones et al.*, 1989]. For this event, during the previous 2 h, IMF B_z is weakly positive (~2 nT) and B_y was negative then increasing to near zero. These IMF conditions result in an expanding duskside oval in the Southern Hemisphere. Precipitating particle data show arcs that are located along the poleward edge of the expanded oval and appear to separate from the auroral oval as B_y increases (becomes less negative)

[23] Figure 5 shows a polar plot with the ST5 satellite track (red line) and DMSP F13 (red) and F15 (green) cross-track plasma flows (plotted in corrected geomagnetic coordinates) from 20 April 2006. DMSP F16 has the same track as F15 but precedes F15 by 9 min. The Sun is toward the top, magnetic local time is denoted by the dashed lines and the lowest latitude is at 60°. The blue cross on the DMSP F16/15 satellite track corresponds to the poleward edge of the expanded duskside oval marked by the vertical line in Figure 6; the black crosses along the DMSP tracks correspond to the particle boundaries associated with the high-latitude arc marked by vertical lines in Figures 7 and 8. The black crosses along the ST5 track mark the boundary of the FAC pair and correspond to the vertical lines in Figure 9. High-latitude arc currents and precipitating particles are located at latitudes poleward of what would normally be the location of the dusk auroral oval.

[24] Figures 6, 7, and 8 show DMSP spectrograms of Southern Hemisphere passes in the dawn-to-dusk direction from DMSP F16, F15, and F13, respectively. Same format as Figure 2 except cross-track horizontal plasma drift data are not available for F16. F16 precedes F15 by 9 min along the same satellite track (see Figure 5). The F16 spectrogram shows an expanded duskside oval (right side of Figure 6) with a thin region of energetic particles at the poleward edge. The energetic particle region at the duskward edge of the auroral oval widens and separates from the oval forming a high-latitude arc as seen in the subsequent passes of DMSP F15 and F13. This arc evolution in the Southern Hemisphere corresponds to negative but increasing IMF B_y

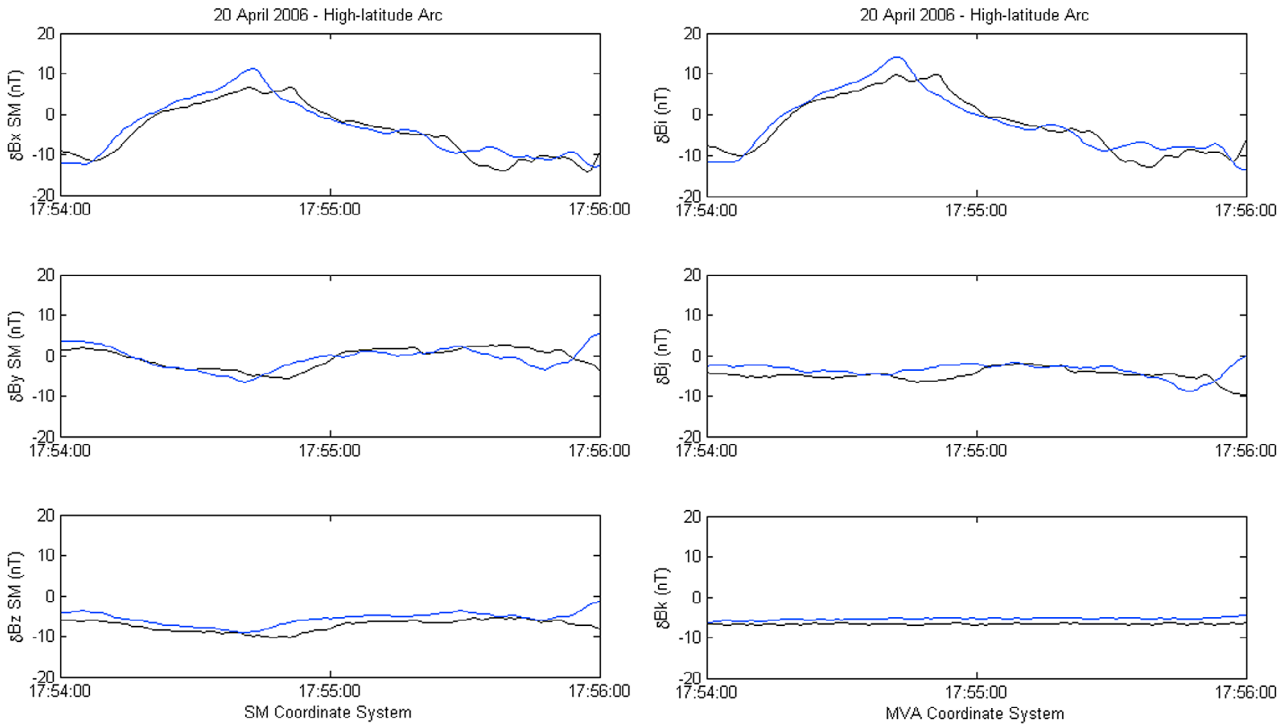

Figure 10. Time-shifted ST5 magnetic field measurements associated with the dusk oval-aligned arc marked by black crosses in Figure 5 and by vertical lines in Figure 9 showing the magnetic field variations in (left) SM coordinates and (right) MVA coordinates. The trailing (ST5-224, blue trace) spacecraft is shifted in time so that measurements taken at the same location are aligned. The time shown is that of the center satellite, ST5-094 (black trace).

and northward IMF. Northern Hemisphere DMSP passes (not shown) show that the dawn oval has expanded poleward similar to the dusk expansion seen in the Southern Hemisphere; this is the expected hemispheric asymmetry when IMF B_y is negative. Subsequent passes in both Northern and Southern hemispheres show that this event remains an oval-aligned transpolar arc and does not move across the polar region. Although data gaps exist at highest latitudes, F15 and F13 measurements show similar cross-track ionospheric plasma flows associated with the arc. These data gaps occur because the ion density has dropped below the instrument sensitivity (<500/cm). In this case, only measurements made at less than ~82° are reliable. The plasma flows are strongly sunward on the duskward part of the oval-aligned arc, and antisunward on the poleward part; magnetic field data (not shown) also show locally balanced field-aligned current pairs. Because of the data gaps, we cannot determine the large-scale convection pattern. However, the currents are locally balanced and their effect on the convection pattern should be localized.

[25] Figure 9 shows ST5 magnetic field measurements from the Southern Hemisphere taken at about the same time as data available from DMSP F16, F15, and F13. The leading (ST5-155, red trace) and trailing (ST5-224, blue trace) spacecraft are shifted in time (631 and 58 s, respectively) so that measurements taken at the same location are aligned. The time shown is that of the center satellite, ST5-094 (black trace). Large changes are seen in the auroral oval FACs measured by ST5 with maximum perturbations in δB_x of ~90 nT. Magnetic field variations along the dawn oval (left side of Figure 9) in the δB_y direction are also quite large (~40 nT). The largest changes in the auroral oval currents occur during the ~10 min interval between ST5-155 and the two trailing spacecraft. On the dawn side (left side of Figure 9) ST5-155 shows there are two upward current sheets poleward of the auroral oval which have a common return current. As these sheets move in opposite directions the return current separates resulting in two current pairs. In the duskside auroral oval (right side of Figure 9) ST5 shows multiple mesoscale variations in the R1 and R2 currents during the ~10–11 min interval between ST5-155 and the trailing spacecraft (ST5-094/224). Even though the largest changes occur in the FACs between ST5-155 and the two trailing spacecraft, there is much more variation between ST5-094 and ST5-224 in the auroral oval than in the high-latitude arc.

[26] A high-latitude arc signature consisting of a single current pair (upward/downward in the dawn-dusk direction) is seen in the ST5 data (marked by vertical lines in Figure 9) at about the same magnetic latitude as those seen in the DMSP precipitating particle data. However, the ST5 pass is on the nightside of the dawn-dusk meridian, while DMSP is on the dayside. The arc signature does not appear in the first ST5 spacecraft (ST5-155), but does appear ~10 min later in the data from the following two spacecraft.

[27] ST5-155 passes through the duskside edge of the expanded auroral oval about 6 min before DMSP F16; ST5-094, ST5-224, F15 and F13 pass through this region about 10, 11, 14 and 28 min after ST5-155, respectively. DMSP F15 and F13 show increasing FAC strength associated with

the high-latitude arc (data not shown). These DMSP measurements which are taken on the dayside of the noon-midnight meridian measure FACs of similar strength but of opposite polarity of those measured by ST5. This is in agreement with the so far unexplained observations of at least partial sunward ionospheric plasma flow along the dayside part of a TPA and antisunward flow along the nightside section [*Nielsen et al.*, 1990; *Eriksson et al.*, 2005; *Liou et al.*, 2005]. This implies that the oval-aligned arc is not formed by a single continuous current sheet but rather one with a common upward current and return currents on either the duskside (dayside part of arc) or dawnside (nightside part).

[28] Figure 10 shows the ST5 magnetic field measured across the high-latitude arc located poleward of the dusk auroral oval (Figure 5) marked by vertical lines in Figure 9. The magnetic field variations in SM coordinates are shown on the left and in MVA coordinates on the right. Large-scale variations are seen mainly in the δB_x and δB_i components. At high latitudes the magnetic field variations consist of a distinct pair of FACs which forms during the ~10 min time period between the first and second ST5 spacecraft; as IMF $|B_z/B_y|$ is increasing. The upward FAC associated with the arc is increasing in strength during the time (~1 min) between ST5-094 and ST5-224. The ratios of the maximum and intermediate variance eigenvalues (e_i/e_j) and the angles the arc makes with the Sun-aligned direction are listed in Table 1, in temporal order. The e_i/e_j ratio for the arc is very large (~20) indicating that an infinite current sheet approximation is valid. The arc has an angle of ~21° with the Sun-aligned direction which is in the range expected for the nightside portion of a dusk oval-aligned arc.

3. Summary and Conclusions

[29] For the first time we are able to analyze changes in field-aligned currents associated with high-latitude transpolar auroral arcs on time scales of a few minutes. This is accomplished through the use of highly accurate multipoint magnetic field measurements provided by the Space Technology 5 mission which consists of three microsatellites in low-Earth orbit (~300–4500 km). Minimum variance analysis is used to determine the appropriateness of the infinite current sheet approximation and to calculate arc alignment angles which are then compared with those estimated from UV images or precipitating particle data in order to determine the validity of using FACs to estimate arc alignment.

[30] The two events presented illustrate changes in high-latitude arcs on time scales of minutes. In the first event we examine measurements of an arc that is part of a highly dynamic auroral pattern, that of a hook-shaped arc. Interesting changes are seen on time scales of 1–3 min. In the second event, a more stable dusk oval-aligned arc is analyzed; still large changes in FACs are seen on time scales of 1–11 min. Both events occur during quiet solar wind conditions when the magnetic field variations measured at Earth are much less than those measured during more active times. Most of the magnetic field variations are seen in the δB_x component. Minimum variance analysis results in large e_i/e_j ratios and indicates that with some confidence we can assume that both of the high-latitude arcs can be represented locally by infinite current sheets.

[31] For event 1 the magnetic field measurements corresponding to the nightside portion of the hook-shaped arc and the dusk oval-aligned arc consist of multiple upward and downward directed mesoscale (~150 km) currents. However, there is very little temporal variation during the 3 min between leading and trailing ST5 satellites compared with the fairly large temporal variations seen in the measurements corresponding to the auroral oval. All three ST5 satellites measure a single field-aligned current pair associated with the dusk oval-aligned arc. Changes seen between ST5-155 and the two following spacecraft include narrowing of the current pair and increasing current density. The calculated angle of the arc with the Sun-aligned direction is consistent with that seen in the GUVI image and is shown to be decreasing in time.

[32] For event 2 large changes are seen in the auroral oval FACs measured during the ~10 min interval between ST5-155 and the two trailing spacecraft. We also see two upward current sheets poleward of the auroral oval with a common return current that evolves such that the return current separates resulting in two current pairs. Overall, the largest changes in the FACs occur between ST5-155 and the two trailing spacecraft, however there is much more variation between ST5-094 and ST5-224 in the auroral oval than in the high-latitude arc. A single field-aligned current pair associated with the dusk oval-aligned arc is seen to form during the ~10 min between the leading and two trailing ST5 satellites. During the time (~1 min) between ST5-094 and ST5-224 the current is increasing in strength. Using MVA we calculate the orientation of the arc which agrees with what is typical for the nightside portion of a dusk oval-aligned transpolar arc.

[33] These events illustrate the dynamic nature of arc formation and show the usefulness of high-resolution multipoint measurements. We also show that MVA is useful in estimating the sheet-like nature of the arc currents and the angle these currents make with the Sun-aligned direction.

[34] **Acknowledgments.** We would like to thank the all the people whose commitment of time and professional expertise have made the ST5 project a success. The authors thank the ACE, IMP 8, and Wind instrument teams for providing magnetometer and plasma data through the GSFC/SPDF OMNIWeb interface at http://omniweb.gsfc.nasa.gov. We also thank the AFRL, Dave Hardy, and Fred Rich for providing the DMSP SSJ4 particle data and the William B. Hanson Center for Space Sciences at the University of Texas at Dallas for providing the DMSP thermal plasma data. The work at the Johns Hopkins University Applied Physics Laboratory was supported by NASA grant NNX07AC57G.

[35] Bob Lysak thanks John Bonnell and two other reviewers for their assistance in evaluating this paper.

References

Baker, K., and S. Wing (1989), A new magnetic coordinate system for conjugate studies at high latitudes, *J. Geophys. Res.*, *94*, 9139, doi:10.1029/JA094iA07p09139.

Blomberg, L. G., and J. A. Cumnock (2005), Electrodynamics of transpolar aurorae, *Adv. Space Res.*, *36*, 1785, doi:10.1016/j.asr.2004.06.022.

Blomberg, L. G., and G. T. Marklund (1993), High-latitude electrodynamics and aurorae during northward IMF, in *Auroral Plasma Dynamics*, *Geophys. Monogr. Ser.*, vol. 80, edited by R. L. Lysak, p. 55, AGU, Washington, D. C.

Bonnell, J., R. C. Elphic, S. Palfery, R. J. Strangeway, W. K. Peterson, D. Klumpar, C. W. Carlson, R. E. Ergun, and J. P. McFadden (1999), Observations of polar cap arcs on FAST, *J. Geophys. Res.*, *104*, 12,669, doi:10.1029/1999JA900085.

Carlson, H. C., and S. W. H. Cowley (2005), Accelerated polar rain electrons as the signature of Sun-aligned arcs in the polar cap during northward IMF conditions, *J. Geophys. Res.*, *110*, A05302, doi:10.1029/2004JA010669.

Craven, J. D., J. S. Murphree, L. A. Frank, and L. L. Cogger (1991), Simultaneous optical observations of transpolar arcs in the two polar caps, *Geophys. Res. Lett.*, *18*, 2297, doi:10.1029/91GL02308.

Crooker, N. U. (1979), Dayside merging and cusp geometry, *J. Geophys. Res.*, *84*, 951, doi:10.1029/JA084iA03p00951.

Cumnock, J. A. (2005), High-latitude aurora during steady northward interplanetary magnetic field and changing IMF B_y, *J. Geophys. Res.*, *110*, A02304, doi:10.1029/2004JA010867.

Cumnock, J. A., J. R. Sharber, M. R. Hairston, R. A. Heelis, and J. D. Craven (1997), Evolution of the global auroral pattern during positive IMF B_z and varying IMF B_y conditions, *J. Geophys. Res.*, *102*, 17,489, doi:10.1029/97JA01182.

Cumnock, J. A., J. F. Spann, G. A. Germany, L. G. Blomberg, W. R. Coley, C. R. Clauer, and M. J. Brittnacher (2000), Polar UVI observations of auroral oval intensifications during a transpolar arc event on December 7, 1996, *Rep. TRITA-ALP-2000-01*, R. Inst. of Technol., Stockholm.

Cumnock, J. A., J. R. Sharber, R. A. Heelis, J. F. Spann, L. G. Blomberg, G. A. Germany, and W. R. Coley (2002), Interplanetary magnetic field control of theta aurora development, *J. Geophys. Res.*, *107*(A7), 1108, doi:10.1029/2001JA009126.

Cumnock, J. A., L. G. Blomberg, I. I. Alexeev, E. S. Belenkaya, S. Y. Bobrovnikov, and V. V. Kalegaev (2006), Simultaneous polar aurorae and modelled convection patterns in both hemispheres, *Adv. Space Res.*, *38*, 1685, doi:10.1016/j.asr.2005.04.105.

Cumnock, J. A., L. G. Blomberg, A. Kullen, T. Karlsson, and K. Å. T. Sundberg (2009), Small-scale characteristics of extremely high-latitude aurora, *Ann. Geophys.*, *27*, 3335, doi:10.5194/angeo-27-3335-2009.

Eriksson, S., et al. (2005), On the generation of enhanced sunward convection and transpolar aurora in the high-latitude ionosphere by magnetic merging, *J. Geophys. Res.*, *110*, A11218, doi:10.1029/2005JA011149.

Frank, L. A., and J. D. Craven (1988), Imaging results from Dynamics Explorer 1, *Rev. Geophys.*, *26*, 249, doi:10.1029/RG026i002p00249.

Frank, L. A., J. D. Craven, J. L. Burch, and J. D. Winningham (1982), Polar views of the Earth's aurora with Dynamics Explorer, *Geophys. Res. Lett.*, *9*, 1001, doi:10.1029/GL009i009p01001.

Frank, L. A., et al. (1986), The theta aurora, *J. Geophys. Res.*, *91*, 3177, doi:10.1029/JA091iA03p03177.

Gusev, M. G., and O. A. Troshichev (1986), Hook-shaped arcs in dayside polar cap and their relationship to the IMF, *Planet. Space Sci.*, *34*, 489, doi:10.1016/0032-0633(86)90087-5.

Gussenhoven, M. S. (1982), Extremely high latitude auroras, *J. Geophys. Res.*, *87*, 2401, doi:10.1029/JA087iA04p02401.

Hones, E. W. J., J. D. Craven, L. A. Frank, D. S. Evans, and P. T. Newell (1989), The horse-collar aurora: A frequent pattern of the aurora in quiet times, *Geophys. Res. Lett.*, *16*, 37, doi:10.1029/GL016i001p00037.

Huang, C. Y., L. A. Frank, W. K. Peterson, D. J. Williams, W. Lennartsson, D. G. Mitchell, R. C. Elphic, and C. T. Russell (1987), Filamentary structures in the magnetotail lobes, *J. Geophys. Res.*, *92*, 2349, doi:10.1029/JA092iA03p02349.

Huang, C. Y., J. D. Craven, and L. A. Frank (1989), Simultaneous observations of a theta aurora and associated magnetotail plasmas, *J. Geophys. Res.*, *94*, 10,137, doi:10.1029/JA094iA08p10137.

Ismail, S., and C.-I. Meng (1982), A classification of polar cap auroral arcs, *Planet. Space Sci.*, *30*, 319, doi:10.1016/0032-0633(82)90037-X.

Kan, J., and W. Burke (1985), A theoretical model of polar cap auroral arcs, *J. Geophys. Res.*, *90*, 4171, doi:10.1029/JA090iA05p04171.

Kullen, A. (2000), The connection between transpolar arcs and magnetotail rotation, *Geophys. Res. Lett.*, *27*, 73, doi:10.1029/1999GL010675.

Kullen, A., and P. Janhunen (2004), Relation of polar auroral arcs to magnetotail twisting and IMF rotation: A systematic MHD simulation study, *Ann. Geophys.*, *22*, 951, doi:10.5194/angeo-22-951-2004.

Kullen, A., M. Brittnacher, J. A. Cumnock, and L. G. Blomberg (2002), Solar wind dependence of the occurrence and motion of polar auroral arcs: A statistical study, *J. Geophys. Res.*, *107*(A11), 1362, doi:10.1029/2002JA009245.

Kullen, A., J. A. Cumnock and T. Karlsson (2008), Seasonal dependence and solar wind control of transpolar arc luminosity, *J. Geophys. Res.*, *113*, A08316, doi:10.1029/2008JA013086.

Le, G., Y. Wang, J. A. Slavin, and R. J. Strangeway (2009), Space Technology 5 multipoint observations of temporal and spatial variability of field-aligned currents, *J. Geophys. Res.*, *114*, A08206, doi:10.1029/2009JA014081.

Liou, K., J. M. Ruohoniemi, P. T. Newell, R. Greenwald, C.-I. Meng, and M. R. Hairston (2005), Observations of ionospheric plasma flows within theta auroras, *J. Geophys. Res.*, *110*, A03303, doi:10.1029/2004JA010735.

Marklund, G. T., and L. G. Blomberg (1991), On the influence of localized electric fields and field-aligned currents associated with polar arcs on the global potential distribution, *J. Geophys. Res.*, *96*, 13,977, doi:10.1029/91JA01120.

Marklund, G. T., L. G. Blomberg, J. S. Murphree, R. D. Elphinstone, L. J. Zanetti, R. E. Erlandson, I. Sandahl, O. de la Beaujardière, H. Opgenoorth, and F. J. Rich (1991), On the electrodynamical state of the auroral ionosphere during northward IMF: A transpolar arc case study, *J. Geophys. Res.*, *96*, 9567, doi:10.1029/90JA02644.

Menietti, J. D., and J. L. Burch (1987), DE 1 observations of theta aurora plasma source regions and Birkeland current charge carriers, *J. Geophys. Res.*, *92*, 7503, doi:10.1029/JA092iA07p07503.

Murphree, J. S., and L. L. Cogger (1981), Observed connections between apparent polar cap features and the instantaneous diffuse auroral oval, *Planet. Space Sci.*, *29*, 1143, doi:10.1016/0032-0633(81)90120-3.

Murphree, J. S., C. D. Anger, and L. L. Cogger (1982), The instantaneous relationship between polar cap and oval auroras at times of northward interplanetary magnetic field, *Can. J. Phys.*, *60*, 349.

Naehr, S. M., and F. R. Toffoletto (2004), Quantitative modeling of the magnetic field configuration associated with the theta aurora, *J. Geophys. Res.*, *109*, A07202, doi:10.1029/2003JA010191.

Nielsen, E., J. D. Craven, L. A. Frank, and R. A. Heelis (1990), Ionospheric flows associated with a transpolar arc, *J. Geophys. Res.*, *95*, 21,169, doi:10.1029/JA095iA12p21169.

Obara, T., T. Mukai, H. Hayakawa, A. Nishida, K. Tsuruda, and H. Fukunishi (1993), Akebono (EXOS D) observations of small-scale electromagnetic signatures relating to polar cap precipitation, *J. Geophys. Res.*, *98*, 11,153, doi:10.1029/92JA01420.

Peterson, W. K., and E. E. Shelley (1984), Origin of the plasma in a cross-polar cap auroral feature (theta aurora), *J. Geophys. Res.*, *89*, 6729, doi:10.1029/JA089iA08p06729.

Slavin, J. A. (2006), Space Technology 5 measurements of the near-Earth magnetic field: Initial results, *Eos Trans. AGU*, *87*(52), Fall Meet. Suppl., Abstract SM14A-05.

Slavin, J. A., G. Le, R. J. Strangeway, Y. Wang, S. A. Boardsen, M. B. Moldwin, and H. E. Spence (2008), Space Technology 5 multi-point measurements of near-Earth magnetic fields: Initial results, *Geophys. Res. Lett.*, *35*, L02107, doi:10.1029/2007GL031728.

Slinker, S. P., J. A. Fedder, D. J. McEwen, Y. Zhang, and J. G. Lyon (2001), Polar cap study during northward interplanetary magnetic field on 19 January 1998, *Phys. Plasmas*, *8*, 1119, doi:10.1063/1.1355680.

Sonnerup, B. U. O., and L. J. Cahill Jr. (1967), Magnetopause structure and attitude from Explorer 12 observations, *J. Geophys. Res.*, *72*, 171, doi:10.1029/JZ072i001p00171.

Sonnerup, B. U. Ö., and M. Scheible (1998), Minimum and maximum variance analysis, in *Analysis Methods for Multi-Spacecraft Data*, *ISSI Sci. Rep. Ser.*, vol. 1, edited by G. Paschmann and P. Daly, p. 185, Eur. Space Agency, Paris.

Toffoletto, F. R., and T. W. Hill (1989), Mapping of the solar wind electric field to the Earth's polar caps, *J. Geophys. Res.*, *94*, 329, doi:10.1029/JA094iA01p00329.

Valladares, C. E., H. C. Carlson, and K. Fukui (1994), Interplanetary magnetic field dependency of stable Sun-aligned polar cap arcs, *J. Geophys. Res.*, *99*, 6247, doi:10.1029/93JA03255.

Wang, Y., G. Le, J. A. Slavin, S. A. Boardsen, and R. J. Strangeway (2009), Space Technology 5 measurements of auroral field-aligned current sheet motion, *Geophys. Res. Lett.*, *36*, L02105, doi:10.1029/2008GL035986.

J. A. Cumnock, Center for Space Sciences, University of Texas at Dallas, MS WT15, PO Box 830688, Richardson, TX 75083-0688, USA. (cumnock@utdallas.edu)

S. Imber, G. Le, and J. A. Slavin, Heliophysics Science Division, NASA Goddard Space Flight Center, Greenbelt, MD 20771, USA.

L. J. Paxton and Y. Zhang, Johns Hopkins University Applied Physics Laboratory, Laurel, MD 20723-6099, USA.